CHEMISTRY
A EUROPEAN JOURNAL

DOI: 10.1002/chem.200500805

Synthesis of Cyano-Bridged Magnetic Nanoparticles Using Room-Temperature Ionic Liquids

Guylhaine Clavel, Joulia Larionova,* Yannick Guari,* and Christian Guérin[a]

Abstract: A principally new exploit of ionic liquids as an alternative reaction medium in the synthesis of cyano-bridged coordination-polymer nanoparticles is reported. Stable colloid solutions containing nanoparticles of cyano-bridged molecule-based magnets, $M_3[Fe(CN)_6]_2$/[RMIM][BF_4] (M^{2+} = Ni, Cu, Co) and $Fe_4[Fe(CN)_6]_3$/[RMIM][BF_4] (R = 1-butyl (BMIM), 1-decyl (DMIM)), were prepared in the corresponding 1-R-3-methylimidazolium tetrafluoroborate [RMIM][BF_4], which acts as both a stabilising agent and a solvent. By varying the length of the N-alkyl chain on the imidazolium cation of $[RMIM]^+$ and the temperature, the growing process can be controlled to produce nanoparticles of different sizes. By studying the magnetic properties of frozen colloids it is shown that the relaxation of magnetisation is strongly influenced by interparticle interactions, which leads to the appearance of spin-glass-like dynamics in these systems.

Keywords: cyanides · ionic liquids · magnetic properties · materials science · nanostructures

Introduction

Room-temperature ionic liquids are a new class of organic solvents, which have received much attention in many fields of chemistry owing to their unique physicochemical properties, such as high fluidity, high thermal stability, low melting temperature, extended temperature range in the liquid state, low toxicity, high ionic conductivity and others.[1] For these reasons, ionic liquids are actively being explored as environmentally benign solvents for organic chemical reactions,[2] separations,[3] electrochemical applications,[4] biopolymers[5] and molecular self-assemblies.[6] In recent years, ionic liquids have also been discovered to be excellent media in the formation and stabilisation of metallic or metal oxide nanosized objects.[7–12]

Cyano-bridged bimetallic nanoparticles with a spin state in the range 100–1000 are nanosized magnetic objects with physical properties intermediate between those of single-molecule magnets[13] and magnetic metallic nanoparticles.[14] The synthesis of these discrete nano-objects and their self-assembly into three-dimensional arrays have attracted increasing interest in the last few years.[15–18] A pioneering work has been realised by S. Mann and co-workers, who prepared cubic nanocrystals (ca. 12–50 nm) of molecular magnetic materials stabilised within reverse micelles.[15] The synthesis of nanosized cyano-bridged magnetic materials with sizes of around 4 nm using reverse micelle media,[16] polymer and biopolymer matrices[17] and amorphous and mesostructured silica[18] have also been reported. Nevertheless, only a few magnetic studies of these materials were described. In this respect, detailed measurements were performed on powdered $Ni_3[Cr(CN)_6]_2$ nanoparticles with a spin ground state of around 130, thus showing that this material has superparamagnetic behaviour with slow magnetisation relaxation.[16]

Here we report a principally new exploit of ionic liquids as an alternative reaction medium in the synthesis of cyano-bridged coordination-polymer nanoparticles of adjustable size. We prepared stable colloid solutions containing nanoparticles of cyano-bridged molecule-based magnets, $M_3[Fe(CN)_6]_2$/[RMIM][BF_4] (M^{2+} = Ni, Cu, Co) and $Fe_4[Fe(CN)_6]_3$/[RMIM][BF_4] (R = 1-butyl (BMIM), 1-decyl (DMIM)), synthesised in the corresponding 1-R-3-methylimidazolium tetrafluoroborate [RMIM][BF_4] (Scheme 1), which acts as both a stabilising agent and a solvent. By varying the length of the N-alkyl chain on the imidazolium

[a] G. Clavel, Dr. J. Larionova, Dr. Y. Guari, Prof. C. Guérin
Laboratoire de Chimie Moléculaire et Organisation du Solide (LCMOS), UMR 5637
Université Montpellier II
Place E. Bataillon, 34095 Montpellier cedex 5 (France)
Fax: (+33) 4-67-14-38-52
E-mail: joulia@univ-montp2.fr
guari@univ-montp2.fr

Supporting information for this article is available on the WWW under http://www.chemeurj.org/ or from the author.

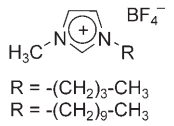

Scheme 1. Molecular structure of 1-R-3-methylimidazolium tetrafluoroborate [RMIM]-[BF_4] in which R = 1-butyl ([BMIM][BF_4]) or 1-decyl ([DMIM][BF_4]).

cation of $[RMIM]^+$ and the temperature, the growing process can be controlled to produce nanoparticles of different sizes.

Results and Discussion

[BMIM][BF_4] and [DMIM]-[BF_4] ionic liquids were chosen as solvents because of their temperature range in the liquid state (melting points at −81 and −25 °C, respectively). $[BMIM]_3[Fe(CN)_6]$ was synthesised by a metathesis reaction from [BMIM][BF_4] and $K_3[Fe(CN)_6]$. Mixing two solutions of $[BMIM]_3[Fe(CN)_6]$ and $[M(H_2O)_6](X)_2$ (M = Cu, X = BF_4; M = Ni, Co, Fe; X = NO_3) in [RMIM][BF_4] for two hours at room temperature led to the formation of a series of deeply coloured and transparent solutions $M_3[Fe(CN)_6]_2$/[RMIM][BF_4] (M = Cu for **1**, Ni for **2**, Co for **3**) and $Fe_4[Fe(CN)_6]_3$/[RMIM][BF_4] (**4**) in which R = 1-butyl for **1a**–**4a** and 1-decyl for **1b**–**4b**

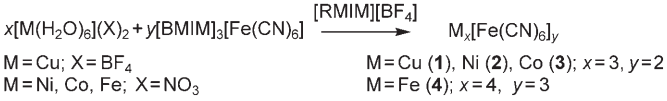

Scheme 2. Synthesis of cyano-bridged molecule-based magnet nanoparticles in [RMIM][BF_4].

(Scheme 2). The as-obtained solutions are stable for months. Nevertheless, adding alcohols (CH_3OH, C_2H_5OH) or water to these solutions induced immediate precipitation of coloured solids.[19] As observed for the bulk materials, UV-visible absorption spectra of the as-obtained solutions **1**–**4** show broad intervalence charge-transfer bands in the visible region (Figure 1, Table 1). However, the maxima of the intervalence bands for the samples are shifted toward higher wavelength from that of the bulk materials by approximately 80 nm for **1a**–**4a** and by approximately 180 nm for **1b**–**4b**. Such shift in UV-visible spectra has also been observed in the case of cyano-bridged nanoparticles incorporated into an amorphous silica matrix[18] and may be ascribed to the surface effect of the nanoparticles.[20] The infrared spectra of solutions **1**–**4** clearly show the bands corresponding to the stretching vibrations of the bridging cyano groups (Table 1).[21]

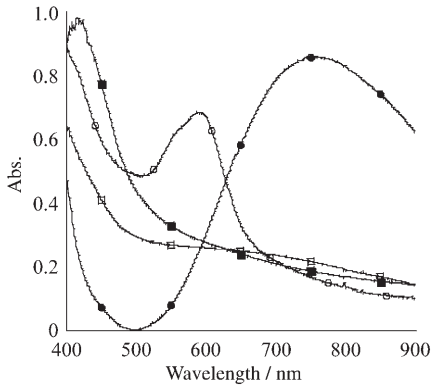

Figure 1. UV/Vis absorption spectra of **1a** (□), **2a** (■), **3a** (○) and **4a** (●).

Drops of solutions **1**–**4** were frozen in liquid nitrogen and sliced using microtomy techniques before being deposited onto a copper grid for transmission electron microscopy (TEM) observations. The TEM images of **1**–**3** show uniformly sized, spherical nanoparticles that are nonaggregated and well dispersed in [RMIM][BF_4]. Figure 2a shows a representative TEM image of **1a** in which nanoparticles with a mean size of 3.3 ± 0.6 nm are observed. The colloids obtained in [BMIM][BF_4] (**1a**–**3a**) present very close nanoparticle size distributions of approximately 3 nm, whereas the mean size of the colloids obtained in [DMIM][BF_4] (**1b**–**4b**) slightly decreases by approximately 0.9 nm (Table 1). This result indicates that the length of the N-alkyl chain on the imidazolium cation of $[RMIM]^+$ has an influence on the nanoparticle size distribution. As observed previously, the processes of nucleation and growth govern the size of the nanoparticles.[22] In the ionic-liquid medium, high nucleation rate due to the low interface tension and weak Ostwald ripening favour the formation of small nanoparticles.[23] In this respect, lower interface tension of [DMIM][BF_4] (26 mJm^{-2} at 336 K) in comparison with [BMIM][BF_4] (38 mJm^{-2} at 336 K) favours the formation of smaller nanoparticles.[24] It is also conceivable that the resulting nanoparticles are constituted of an anionic coordination-polymer network electrostatically complexed by imidazolium cations. As a consequence, the alkyl-chain-length modification of the imidazolium cations used as solvent can affect the size of the resulting nanoparticles.

The TEM images of the homometallic sample **4a** are different from the above-mentioned TEM images in that they show the formation of dendritic structures (Figure 2b). Most of the cyano-bridged nanoparticles stick together to form dendrites, and some single nanoparticles disperse evenly in solution. On the other hand, the same nanoparticles formed in ionic liquid [DMIM][BF_4] (thus forming **4b**) are nearly uniformly sized, spherical and well-dispersed. The average diameter of the particles is 2.2 ± 0.6 nm, and no dendrites could be observed. Visibly, in the case of **4a**, [BMIM][BF_4] influences the growth rate on various faces leading to anisotropic nanoparticles, which induces the formation of dendritic structure.[23]

The reaction temperature has a significant influence on the size of the nanoparticles. $[BMIM]_3[Fe(CN)_6]$ reacts with $[M(H_2O)_6](X)_2$ to form nanoparticles even between −50 °C and room temperature. The size distribution of the nanoparticles formed in this temperature range does not change significantly. However, if the mixing of the reactants takes place at 80 °C, the formation of solids consisting of $M_3[Fe(CN)_6]_2$ crystallites of micrometric size with regular

Table 1. Some relevant characteristics of colloids **1**–**4**.

	T [°C]	IR $\tilde{\nu}$(C≡N) [cm^{-1}]	UV/Vis λ [nm]	Nanoparticle size [nm]
$Cu_3[Fe(CN)_6]_2$/[BMIM][BF_4] (**1a**)	RT	2162, 2091 (s)	615	3.3 ± 0.6
$Cu_3[Fe(CN)_6]_2$/[DMIM][BF_4] (**1b**)	RT	2166 (s), 2093	790	2.2 ± 0.7
$Cu_3[Fe(CN)_6]_2$/[BMIM][BF_4] (**1c**)	50	2162, 2091 (s)	615	3.0 ± 0.8
$Cu_3[Fe(CN)_6]_2$/[BMIM][BF_4] (**1d**)	80	2162, 2091 (s)	615	2.4 ± 0.5
$Ni_3[Fe(CN)_6]_2$/[BMIM][BF_4] (**2a**)	RT	2159 (s), 2085	415 (sh)	2.7 ± 0.4
$Ni_3[Fe(CN)_6]_2$/[DMIM][BF_4] (**2b**)	RT	2161 (s), 2089	460 (sh)	1.9 ± 0.8
$Co_3[Fe(CN)_6]_2$/[BMIM][BF_4] (**3a**)	RT	2158, 2084(s)	590	3.0 ± 0.8
$Co_3[Fe(CN)_6]_2$/[DMIM][BF_4] (**3b**)	RT	2155, 2086 (s)	630	2.3 ± 0.6
$Fe_4[Fe(CN)_6]_3$/[BMIM][BF_4] (**4a**)	RT	2073 (s)	760	dendrite, 3.0 ± 0.7
$Fe_4[Fe(CN)_6]_3$/[DMIM][BF_4] (**4b**)	RT	2102, 2049 (s)	880	2.2 ± 0.6

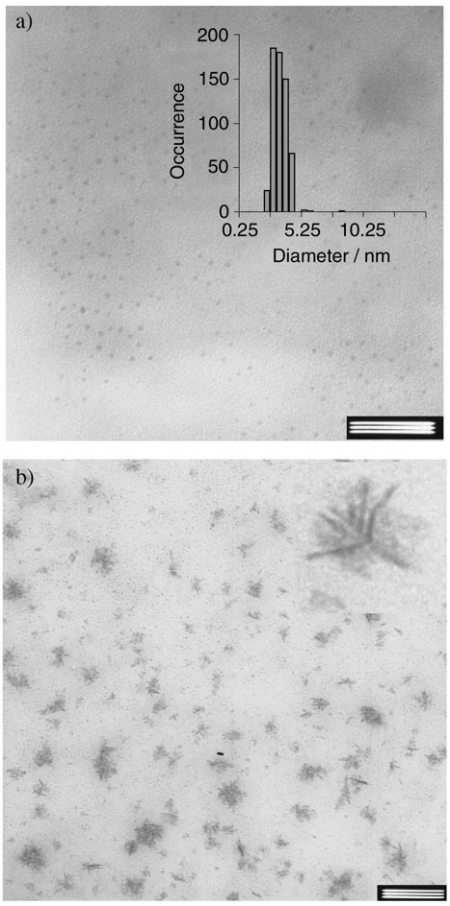

Figure 2. a) TEM image of solution **1a** (scale bar = 50 nm); inset: size-distribution histogram for **1a**. b) TEM micrograph of solution **4a** (scale bar = 50 nm); inset: magnification of the TEM image of **4a**.

geometrical shape were observed. These crystallites can be detected by X-ray diffraction techniques.

We also investigated the influence of the postsynthetic heating of the colloids on the nanoparticle size. When, immediately after mixing $[BMIM]_3[Fe(CN)_6]$ with $[M(H_2O)_6](X)_2$ in [BMIM][BF_4], the colloids were heated at 50 or 80 °C for two hours, the solutions maintain their transparency and no visible change of the colloids' aspect was observed. The TEM observations performed on these samples show the presence of uniformly sized, spherical and well-dispersed nanoparticles, as observed in the case of nonheated colloids. However, the size distributions demonstrate that the mean size of the nanoparticles **1a** decreases from 3.3 ± 0.6 nm to 3.0 ± 0.8 and 2.4 ± 0.5 nm after heating at 50 (**1c**) and 80 °C (**1d**), respectively (Table 1). Aggregation of the nanoparticles and the formation of a blue-grey precipitate from the colloids was observed when the temperature was increased to 140 °C.

The magnetic properties of the obtained colloids **1**–**4** studied by direct current (dc) and alternating current (ac) modes are qualitatively different from their bulk counterparts (see Table 2 and the Supporting Information).[25] Figure 3 shows

Table 2. Some relevant magnetic data for colloids **1**–**3**.

	Concentration [M]	T_B [K]	Δ/k_B [K]	τ_0 [s]	z	H_c at 1.8 K [Oe]
1a	1.4×10^{-6}	5.5	191	3.0×10^{-18}	8.2	582
1a	7.4×10^{-7}	5.2	185	1.6×10^{-18}	7.1	600
1a	1.8×10^{-7}	4.3	137	1.7×10^{-15}	–[a]	607
1b	1.4×10^{-6}	5.1	160	5.7×10^{-17}	7.5	600
1d	1.4×10^{-6}	3.1	115	5.4×10^{-17}	7.1	–
2a	1.4×10^{-6}	5.2	219	2.6×10^{-21}	6.5	688
2b	1.4×10^{-6}	4.7	166	2.6×10^{-18}	8.8	690
3a	1.4×10^{-6}	2.3	52	5.7×10^{-13}	–[a]	–
3b	1.4×10^{-6}	< 1.8	–	–	–	–

[a] Could not be fitted.

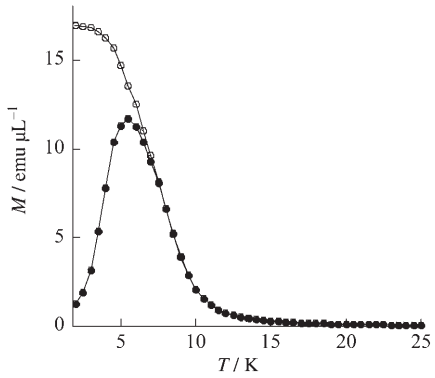

Figure 3. FC (○)/ZFC (●) magnetisation curves for **1a** performed with an applied field of 10 Oe.

the field-cooled/zero-field-cooled (FC/ZFC) magnetisation (M) results in the range of 1.8–25 K for sample **1a**.[26] The ZFC curve shows a narrow peak at 5.5 K, which indicates the blocking temperature (T_B) of the particles with a mean volume. The FC curve increases as the temperature decreas-

es and reaches saturation at 3 K. The FC and ZFC curves coincide at high temperatures and start to separate at 7 K; this indicates the blocking temperature of the largest particles. The closeness of T_B to the separation temperature of the ZFC/FC curves (T_{sep}) indicates the presence of nanoparticles with a narrow energy-barrier distribution.[27] The FC/ZFC curves of sample **1b** present similar shapes and show a blocking temperature of 5.1 K.

To investigate the nature of the irreversibility observed in the FC/ZFC curves in more detail, the temperature dependence of the alternating current (ac) susceptibility was studied. The temperature dependence of the in-phase (χ') and out-of-phase (χ'') components of ac susceptibility for **1a** measured in a zero external field with different frequencies ranging from 1 to 1500 Hz is shown in Figure 4. At 1 Hz, both χ' and χ'' responses exhibit a peak at 6.2 and 5.0 K, respectively, which shift towards higher temperature when the frequency increases. The frequency dependence of these peaks can be analysed by the Arrhenius law, shown in Equation (1):

$$\tau = \tau_0 \exp(\Delta/k_B T) \quad (1)$$

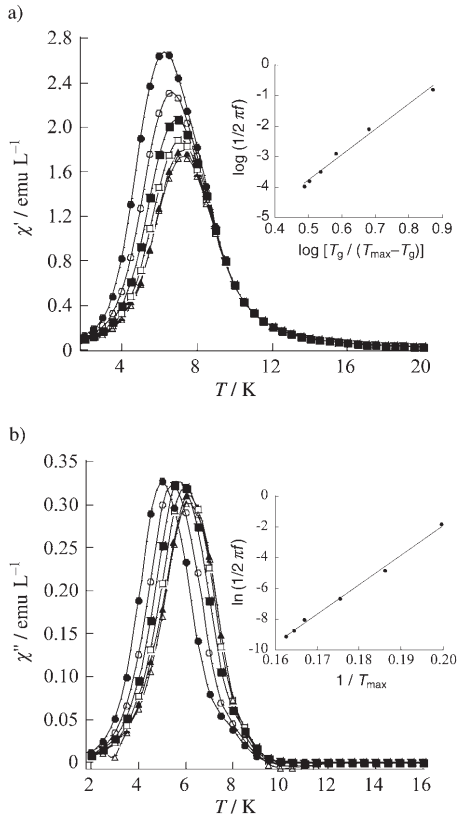

Figure 4. a) Temperature dependence of the in-phase (χ') component of the ac susceptibility of **1a**; inset: thermal variation of the relaxation time according to a power law. b) Temperature dependence of the out-of-phase (χ'') component of the ac susceptibility of **1a**; inset: thermal variation of the relaxation time according to the Arrhenius law. Frequencies: 1 (●), 20 (○), 125 (◆), 499 (□), 998 (▲) and 1488 Hz (▽).

in which Δ is the average energy barrier and is given by $\Delta = KV$ (K being the anisotropy energy constant and V the particle volume). The energy barrier Δ/k_B and the pre-exponential factor τ_0 were estimated to be 191 K and 3.0×10^{-18} s, respectively (inset of Figure 4b). This low value of τ_0 is close to what is commonly observed for spin glass rather than for superparamagnetic systems, which is usually in the range 10^{-10}–10^{-12} s.[28] Sample **1b** exhibits similar behaviour with a smaller energy barrier of 160 K and τ_0 of 5.7×10^{-17} s. The presence of magnetic interparticle interactions along with surface effects can affect the dynamics of magnetisation reorientation and give rise to the appearance of spin-glass-like dynamics.[29] On the other hand, it cannot be excluded that the observed behaviour of our colloids is a result of the glasslike behaviour of a single particle due to the small size of the particles and hence to the particularly relevant role of the surface.[27,30] From the average particle-energy-barrier values and by using the average particle-volume values obtained from TEM measurements, we evaluated the anisotropy constant K, which is equal to 5.9×10^5 and 3.9×10^5 Jm^{-3} for **1a** and **1b**, respectively. These values are in the range of the K values observed for metal oxide nanoparticles.[27] To check if the relaxation time in the obtained frozen colloids presents a critical slowing down, we performed a dynamic scaling analysis according to the power law shown in Equation (2):

$$\tau = \tau_0[T_g/(T_{max}-T_g)]^z \quad (2)$$

where T_g is the glass temperature and z is the critical exponent, which is commonly used in classical spin-glass systems.[31] The frequency dependence of the maximum of the ac susceptibility of **1a** was satisfactorily fitted with $T_g = 5.5$ K, $\tau_0 = 1.3\times10^{-8}$ s and $z = 8.2$, the latter being similar to the exponent reported for spin glasses (inset of Figure 4a).[29]

To further investigate the influence of interparticle interactions on the magnetic relaxation in our system, we performed ac susceptibility measurements with varying nanoparticle concentration and thus with varying interparticle interaction strength.[32] The temperature dependence of the ac susceptibility for **1a** was measured for three different concentrations: 1.4×10^{-6}, 7.4×10^{-7} and 1.8×10^{-7} M. With decreasing concentration, the peaks of the χ' and χ'' components were shifted to lower temperatures (Figure 5), which suggests that the blocking temperature, and most likely the energy barrier, decreases with decreasing interparticle interactions. In addition, the Arrhenius law fitting of the thermal variation of the relaxation time performed for this series of samples shows that the energy barrier Δ/k_B decreases with decreasing interaction strength (Table 2). These features are in accord with studies performed on strongly interacting particles in frozen ferrofluids.[32] On the other hand, the thermal variation of the relaxation time of the most diluted sample (1.8×10^{-7} M) cannot be satisfactory fitted with a power law, visibly suggesting that the decrease of interparticle interactions within our series of concentrations leads to the change

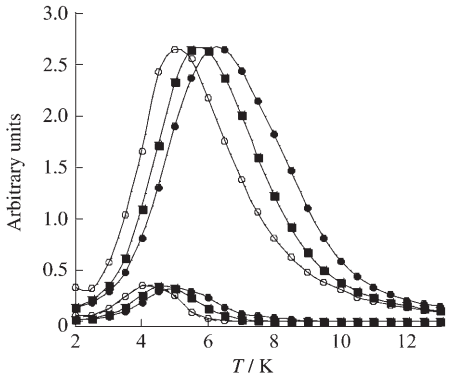

Figure 5. Temperature dependence of the in-phase (χ') and out-of-phase (χ'') components of the ac susceptibility measured with frequency of 1 Hz for colloid **1a** with varying concentration: 1.4×10^{-6} (●), 7.4×10^{-7} (■) and 1.8×10^{-7} M (○).

of the magnetic regime from spin-glass-like dynamics to a superparamagnetic regime modified by interparticle interactions.[31]

The field dependence of the magnetisation for samples **1a** and **1b** at 2 K shows saturation-magnetisation values of 27366 and 27389 emu mol^{-1} (4.9 μ_B), respectively, which correspond to the expected value for a $\{Cu_3Fe_2\}$ unit with ferromagnetic Cu^{2+}–Fe^{3+} interactions through the cyano bridge.[33] A hysteresis effect is observed at this temperature with a coercive field (H_c) of 582 and 600 Oe, respectively (Figure 6, Table 2). An S-shape of the first magnetisation

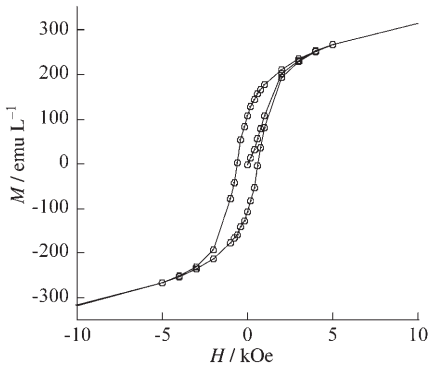

Figure 6. Field dependence of the magnetisation for **1a**, performed at 1.8 K.

curve is in agreement with the presence of strong interparticle interactions in the system.[30,34]

To obtain evidence of the influence of the nanoparticle size on the magnetic properties of the colloids, the magnetic measurements were performed on sample **1d**, which was obtained after heating at 80 °C (nanoparticle mean size = 2.4 ± 0.5 nm), and compared with sample **1a** (nanoparticle mean size = 3.3 ± 0.6 nm). The ZFC magnetisation curve of **1d** shows a narrow peak situated at 3.1 K (5.5 K for **1a**), which suggests that the blocking temperature of particles with a mean volume decreases as the size of the nanoparticles decreases. The temperature dependence of the in-phase (χ') and out-of-phase (χ'') components of the ac susceptibility for **1d** measured with different frequencies ranging from 1 to 1500 Hz exhibit frequency dependent peaks, which shift towards higher temperature when the frequency increases. The thermal variation of the relaxation time fitted with the Arrhenius law gives an average energy barrier (Δ/k_B) of 115 K and pre-exponential factor (τ_0) of 5.4×10^{-17} (Table 2). These results clearly show that the size of the nanoparticles affects the average energy barrier of the system and that decreasing the nanoparticle size induces a decrease of the energy barrier.[30]

Conclusion

In summary, we have developed a method for the synthesis of heterometallic cyano-bridged coordination polymers of controlled size, in ionic liquids employed as both structuring agents and solvents. To the best of our knowledge, this is the first report of the use of ionic liquids in the synthesis of coordination-polymer nanoparticles of adjustable size. Deeply coloured colloids containing uniformly sized, spherical nanoparticles with small sizes of approximately 2–3 nm were obtained. These colloidal systems of nanoparticles/ionic liquid are exceptionally stable and no ligand is required, which suggests that the ionic liquid plays the role of stabilising agent. We observed that the length of the N-alkyl chain on the imidazolium cation of the ionic liquid influences the size of the nanoparticles, which slightly decreases as the length of the alkyl chain increases. The nanoparticle size can also be changed by controlling the temperature. It is noteworthy that, in one case, the nanoparticles stick together to form dendritic structures. The study of the magnetic properties of frozen colloids shows that the relaxation of magnetisation is strongly influenced by interparticle interactions, which leads to the appearance of spin-glass-like dynamics in these systems.

Experimental Section

General: $K_3[Fe(CN)_6]$ was purchased from Acros and $[Ni(H_2O)_6](NO_3)_2$, $[Co(H_2O)_6](NO_3)_2$, $[Cu(H_2O)_4](BF_4)_2$ and $[Fe(H_2O)_6](NO_3)_2$ were purchased from Aldrich. $AgBF_4$ was purchased from Alfa Aesar. [BMIM]-$[BF_4]$[35] and [DMIM]$[BF_4]$[36] were synthesised according to published procedures. The quantity of water was controlled by the Karl–Fisher method and maintained at 0.2 wt % for all syntheses.

IR spectra were recorded on a Perkin–Elmer 1600 spectrometer with 4 cm^{-1} resolution. UV/Vis spectra were recorded on a Cary 5E spectrometer in solution or in the solid state on KBr disks. Transmission electron microscopy (TEM) observations were carried out at 100 kV (JEOL 1200 EXII). Samples for TEM measurements were prepared by using ultramichrotomy techniques from a frozen drop of solution or from resin-embedded powder for solid materials and then deposited onto copper grids. Magnetic susceptibility data were collected with a Quantum Design MPMS-XL SQUID magnetometer. The data were corrected for the sample holder and the diamagnetism contributions were calculated from the Pascal constants.[37]

Synthesis of $[BMIM]_3[Fe(CN)_6]$: A methanolic solution (100 mL) of $K_3[Fe(CN)_6]$ (1 g, 3 mmol) and $[BMIM][BF_4]$ (2 g, 9 mmol) were mixed and stirred for one night at room temperature. The suspension was filtered off, the filtrate was concentrated (ca. 10 mL) and the product was precipitated by addition of Et_2O. $[BMIM]_3[Fe(CN)_6]$ was obtained as a yellow powder in 94% yield. IR (KBr): $\tilde{\nu}=3150$ (NCH of NC(H)), 3096 (ring $HCCH_{as}$), 2933 (HCH_{sym} of $CH_3(N)$), 2115 (CN), 1574 (CH_3N, CH_2N, CH_2N of ring in plane), 1467 (δ(HCH) of $CH_3(N)$), 1170 (CH_3N, CH_2N, CH_2N of ring in plane), 628 cm^{-1} (CH_3N, CH_2N, CH_2N of ring out of plane); elemental analysis calcd (%) for $C_{30}FeH_{15}N_{12}$: C 57.25, Fe 8.88, N 26.71; found: C 57.41, Fe 8.19, N 26.59.

Synthesis of colloids $M_3[Fe(CN)_6]_2$/[RMIM][BF_4] (M = Cu for 1, Ni for 2, Co for 3) and $Fe_4[Fe(CN)_6]_3$/[RMIM][BF_4] (R = 1-butyl for 1a–4a and 1-decyl for 1b–4b): In a typical synthesis, a solution of $[M(H_2O)_6](X)_2$ (X = NO_3 for **1**, **3**, **4** and BF_4 for **2**) (0.22 mmol) in [RMIM][BF_4] (1 mL) was added to a solution of $[BMIM]_3[Fe(CN)_6]$ (0.15 mmol) in [RMIM][BF_4] (1.5 mL). The yellow solutions change colour without any visible precipitate. After 5 min, the solutions was stirred for 2 h at room temperature for **1a**,**b**–**4a**,**b** and at 50 and 80 °C for **1c** and **1d**, respectively.

Dilution of the colloids: Colloid **1a** with a concentration of 1.4×10^{-6} M was diluted with [BMIM][BF_4] two and four times in order to obtain the concentrations 7.4×10^{-7} and 1.8×10^{-7} M, respectively.

Acknowledgements

The authors thank C. Reibel (LPMC, Montpellier, France) for the magnetic measurements. This work was supported by the European Network of Excellence MagmaNet.

[1] a) P. Wasserscheid, W. Keim, *Angew. Chem.* **2000**, *112*, 3926–3945; *Angew. Chem. Int. Ed.* **2000**, *39*, 3772–3789; b) T. Welton, *Chem. Rev.* **1999**, *99*, 2071–2083; c) A. Bosmann, G. Francio, E. Janssen, M. Solinas, W. Leitner, P. Wasserscheid, *Angew. Chem.* **2001**, *113*, 2769–2771; *Angew. Chem. Int. Ed.* **2001**, *40*, 2697–2699; d) L. A. Blanchard, D. Hancu, E. J. Beckman, J. F. Brennecke, *Nature* **1999**, *399*, 28–29.

[2] a) P. Wasserscheid, T. Welton, *Ionic Liquids in Synthesis*, Wiley-VCH, Weinheim **2003**; b) R. Scheldon, *Chem. Commun.* **2001**, 2399–2407.

[3] J. G. Huddleston, H. D. Willauer, R. P. Swatloski, A. E. Visser, R. D. Rogers, *Chem. Commun.* **1998**, 1765–1766.

[4] a) A. B. McEwen, S. F. McDevitt, V. R. Koch, *J. Electrochem. Soc.* **1997**, *144*, 3392–3397; b) E. V. Dickinson, M. E. Williams, S. M. Hendrickson, H. Masui, R. W. Murray, *J. Am. Chem. Soc.* **2001**, *123*, 218–222.

[5] a) N. Kimizuka, T. Nakashima, *Langmuir* **2001**, *17*, 6759–6761; b) R. P. Swatloski, S. K. Spear, J. D. Holbrey, R. D. Rogers, *J. Am. Chem. Soc.* **2002**, *124*, 4974–4975.

[6] T. Nakashima, N. Kimizuka, *Chem. Lett.* **2002**, 1018–1019.

[7] a) G.-T. Wei, Z. Yang, C.-Y. Lee, H.-Y. Yang, C. R. Chris Wang, *J. Am. Chem. Soc.* **2004**, *126*, 5036–5037; b) H. Itoh, K. Naka, Y. Chujo, *J. Am. Chem. Soc.* **2004**, *126*, 3026–3027; c) K.-S. Kim, D. Demberelnyamba, H. Lee, *Langmuir* **2004**, *20*, 556–560.

[8] J. Dupont, G. S. Fonseca, A. P. Umpierre, P. F. P. Fichtner, S. R. Teixeira, *J. Am. Chem. Soc.* **2002**, *124*, 4228–4229.

[9] C. W. Scheeren, G. Machado, J. Dupont, P. F. P. Fichtner, S. R. Texeira, *Inorg. Chem.* **2003**, *42*, 4738–4742.

[10] a) J. Huang, T. Jiang, B. Han, H. Gao, Y. Chang, G. Zhao, W. Wu, *Chem. Commun.* **2003**, 1654–1655; b) V. Calo, A. Nacci, A. Monopoli, S. Laera, N. Cioffi, *J. Org. Chem.* **2003**, *68*, 2929–2933; c) R. R. Deshmukh, R. Rajagopal, K. V. Srinivasan, *Chem. Commun.* **2001**, 1544–1545.

[11] Y.-J. Zhu, W.-W. Wang, R.-J. Qi, X.-L. Hu, *Angew. Chem.* **2004**, *116*, 1434–1438; *Angew. Chem. Int. Ed.* **2004**, *43*, 1410–1414.

[12] T. Nakashima, N. Kimizuka, *J. Am. Chem. Soc.* **2003**, *125*, 6386–6387.

[13] D. Gatteschi, R. Sessoli, *Angew. Chem.* **2003**, *115*, 278–309; *Angew. Chem. Int. Ed.* **2003**, *42*, 268–297.

[14] a) K. J. Klabunde, *Nanoscale Materials in Chemistry*, Wiley-Interscience, New York, **2001**; b) R. C. O'Handley, *Modern Magnetic Materials*, Wiley-Interscience, New York, **1999**.

[15] a) S. Vaucher, M. Li, S. Mann, *Angew. Chem.* **2000**, *112*, 1863–1866; *Angew. Chem. Int. Ed.* **2000**, *39*, 1793–1796; b) S. Vaucher, J. Fielden, M. Li, E. Dujardin, S. Mann, *Nano Lett.* **2002**, *2*, 225–229; c) E. Dujardin, S. Mann, *Adv. Mater.* **2004**, *16*, 1125–1129.

[16] L. Catala, T. Gacoin, J.-P. Boilot, E. Riviere, C. Paulsen, E. Lhotel, T. Mallah, *Adv. Mater.* **2003**, *15*, 826–829.

[17] a) J. M. Dominguez-Vera, E. Colacio, *Inorg. Chem.* **2003**, *42*, 6983–6985; b) T. Uemura, S. Kitagawa, *J. Am. Chem. Soc.* **2003**, *125*, 7814–7815.

[18] a) G. Clavel, Y. Guari, J. Larionova, Ch. Guerin, *New J. Chem.* **2005**, *29*, 255–279; b) J. G. Moore, E. J. Lochner, C. Ramsey, N. S. Dalal, A. E. Stiegman, *Angew. Chem.* **2003**, *115*, 2847–2849; *Angew. Chem. Int. Ed.* **2003**, *42*, 2741–2743.

[19] TEM measurements show that these solids consist of aggregated nanoparticles and crystallites of micrometric size with regular geometrical shape as truncated triangular prisms or cubes (edge length of around 50 nm).

[20] D. L. Feldheim, C. A. Foss, *Metal Nanoparticles*, Marcel Dekker, New York, **2002**.

[21] K. Nakamoto, *Infrared and Raman Spectra*, Wiley, New York, **1986**.

[22] B. L. Cushing, V. L. Kolesnichenko, C. J. O'Connor, *Chem. Rev.* **2004**, *104*, 3893–3946.

[23] M. Antonietti, D. Kuang, B. Smarsly, Y. Zhou, *Angew. Chem.* **2004**, *116*, 5096–5100; *Angew. Chem. Int. Ed.* **2004**, *43*, 4988–4992.

[24] G. Law, P. R. Watson, *Langmuir* **2001**, *17*, 6138–6141.

[25] The bulk cyano-bridged molecule-based magnets of formula $M_3[Fe(CN)_6]_2$ (M = Cu, Ni, Co,) and $Fe_4[Fe(CN)_6]_3$ show a long-range magnetic ordering below their critical temperatures, which are equal to 21, 23, 14 and 5.6 K, respectively. The temperature dependence of the χ' and χ'' components of ac susceptibility show no frequency-dependent peak. For instance, see: a) F. Herren, P. Fischer, A. Lüdi, W. Hälg, *Inorg. Chem.* **1980**, *19*, 956–959; b) V. Cadet, M. Bujoli-Doeuff, L. Force, M. Verdaguer, K. E. Malkhi, A. Deroy, J. P. Besse, C. Chappert, P. Veillet, J. P. Renard, P. Beauvillain in *Magnetic Molecular Materials, NATO ASI Series E, Vol. 198* (Eds.: D. Gatteschi, O. Kahn, J. S. Miller, F. Palacio), Kluwer, Dordrecht, **1991**, p. 281; c) W. R. Entley, C. R. Treadway, G. S. Girolami, *Mol. Cryst. Liq. Cryst.* **1995**, *273*, 591–604.

[26] The ZFC measurements were recorded by heating the sample under an applied magnetic field of 10 Oe followed by cooling the sample in a zero magnetic field. The FC measurements were recorded by cooling the sample below the magnetic field of 10 Oe. The irreversibility observed in the FC/ZFC curves can be attributed to the characteristic blocking–unblocking process of the particle magnetic moment when thermal energy is varied. As the relaxation time of a magnetic particle increases with decreasing temperature, we can define, for a certain observation time, a characteristic average temperature, called blocking temperature (T_B), below which the particle moment appears blocked on the timescale of the experiment.

[27] D. Bonacchi, A. Caneschi, D. Dorignac, A. Falqui, D. Gatteschi, D. Rovai, C. Sangregorio, R. Sessoli, *Chem. Mater.* **2004**, *16*, 2016–2020.

[28] D. Fiorani, J. L. Dormann, J. L. Tholence, L. Bessais, D. Villers, *J. Magn. Magn. Mater.* **1986**, *54–57*, 173–174.

[29] P. E. Jonsson, J. L. Garcia-Palacios, M. F. Hansen, P. Nordblad, *J. Mol. Liq.* **2004**, *114*, 131–135.

[30] E. Tronc, D. Fiorani, M. Noguès, A. M. Testa, F. Lucari, F. D'Orazio, J. M. Grenèche, W. Wernsdorfer, N. Galvez, C. Chanéac, D. Mailly, J. P. Jolivet, *J. Magn. Magn. Mater.* **2003**, *262*, 6–14.

[31] J. L. Dormann, R. Cherkaoui, L. Spinu, M. Noguès, F. Lucari, F. D'Orazio, D. Fiorani, A. Garcia, E. Tronc, J. P. Jolivet, *J. Magn. Magn. Mater.* **1998**, *187*, L139–L144.

[32] J. L. Dormann, L. Spinu, E. Tronc, J. P. Jolivet, F. Lucari, F. D'Orazio, D. Fiorani, *J. Magn. Magn. Mater.* **1998**, *183*, L255–L260.
[33] The magnetic moment of 140 μ_B for a particle of **1a** containing 84 Cu^{2+} and 56 Fe^{3+} {$Cu_{84}Fe_{56}$} was obtained as previously described in ref. [16].
[34] P. Zhang, F. Zuo, F. K. Urban, III, A. Khabari, P. Griffiths, A. Hosseini-Tehroni, *J. Magn. Magn. Mater.* **2001**, *225*, 337.
[35] P. A. Z. Suarez, J. E. L. Dullios, S. Einloft, R. F. de Scuza, *Polyhedron* **1996**, *15*, 1217–1219.
[36] J. D. Holbrey, K. R. Seddon, *J. Chem. Soc. Dalton Trans.* **1999**, 2133–2140.
[37] *Theory and Applications of Molecular Paramagnetism* (Eds.: E. A. L. Boudreaux, N. Mulay), Wiley, New York, **1976**.

Received: July 13, 2005
Revised: November 9, 2005
Published online: February 23, 2006

